

Real-time high spatial resolution, in vivo corneal imaging: current successes and future needs

H. Dwight Cavanagh and W.M. Petroll

Department of Ophthalmology, The University of Texas Southwestern Medical Center at Dallas, Dallas, Texas, 5323 Harry Hines Blvd., Dallas, TX, 75390-9057

ABSTRACT

Purpose: To identify, characterize, and discuss the current technological status of in vivo corneal diagnostic imaging and target high-priority future development needs.

Methods: In vivo tandem scanning microscopy (non-coherent), scanning slit confocal microscopy (non-coherent), and laser scanning confocal microscopy (coherent) are examined. The current and future roles of multi-photon and higher order harmonic imaging are also discussed.

Results and Conclusions: This keynote review demonstrates the current abilities and limitations of three currently used clinical imaging modalities to resolve the cellular and structural layers of the cornea temporally and spatially in three or four dimensions (x, y, z, t), with applications to the study of clinical-pathological processes such as inflammation; infection, wound healing, drug toxicity, organ development, differentiation and effects of genetic diseases. Each of these approaches has strengths and weaknesses. Thus, future technological development is essential to provide exciting new insights into understanding the structure and function of not only the cornea and the other ocular structures, but also other multicellular organs in health and disease. These imaging paradigms are among the most important advances in medical science in the past three decades.

Key Words: confocal microscopy, non-invasive imaging, in vivo microscopy, corneal imaging

The invention of the microscope provided a unique method to explore the biological realm of the very small. Observations of the birth, life and death processes of living cells within multicellular organisms were initially limited by the rapidity of movement of physiological processes, and the lack of resolution caused by the thickness or opacity of the tissues viewed. To resolve these problems, tissue excision, fixation, and thin-sectioning prior to viewing were developed, thus providing images unconnected in time whose interpretation was always potentially flawed by sample preparation artifacts. In the past 30 years, in vivo confocal microscopy, a new imaging paradigm has been developed that can overcome these limitations, liberating the dynamic potential of the microscope to view microphysiological processes in situ at high spatial resolution, contrast and magnification.

In this review, the power of current confocal technology to resolve a variety of important clinical and biological questions in the cornea is presented. Current limitations are identified, and the need for future technological development is addressed.

THE OPTICAL PRINCIPLES OF CONFOCAL MICROSCOPY

In 1957, Minsky¹ described the first confocal microscope with optics that restricted the final image seen to light coming only from the focal volume defined by the numerical aperture, magnification, and working distance of the objective lens. This was accomplished by focusing the light source within a small area of the specimen and then focusing the objective lens on the same area. Because both condenser and objective lenses have the same focal point, the microscope was termed *confocal*.

Since Minsky's original instrument, the optical theory of confocal microscopy has been more formally developed and extended by Wilson and Sheppard² and Sheppard and Cogswell.³ In most modern confocal microscopes, a point (i.e., optically diffraction limited) light source is focused onto a small volume within the specimen, and a

confocal point detector is used to collect the resulting signal. This results in a reduction of the amount of out-of-focus signal from above and below the focal plane, which contributes to the detected image and produces a marked increase in both lateral (x, y) and axial (z) resolution, as well as contrast. Because only one tiny volume element of the specimen is observed by each point source/detector element (trading field of view for enhanced resolution), a useful, full field of view must be regained by mechanically scanning. This is achieved by either moving the specimen or by a synchronous movement of the illuminator and detector. Thus, the temporal resolution (t) of the microscope is defined by the speed at which the single x-y field can be produced and recorded. Most important, by varying the plane of focus of both source and detector within the tissue, the specimen can be optically sectioned noninvasively. This remarkable property allows a true paradigm shift in the ability to image microphysiologic processes in situ at magnifications sufficient to resolve cellular and subcellular details as they occur.

Because of consideration for retinal toxicity, the light source used to achieve either point or slit illumination for clinical confocal microscopy was initially restricted to white light in all FDA-approved ophthalmic instruments. Recently, a coherent light source has also been approved (diode laser, 670 nm).

The first practical application of confocal optical theory to the eye was the development in 1974 of the specular microscope by David Maurice, who demonstrated the enhanced resolution and contrast in images obtained by narrowing a slit beam, thus reducing the volume of scattered light contributing to the final image, an optical principle identical to diffraction-limited pinhole (source/detector) confocal imaging.⁴

The design of the objective lens for confocal microscopes is also critical. The z-axis resolution (actual volume element visualized) under confocal conditions is highly dependent on the numerical aperture and higher magnification lenses. However, commercially available, high numerical aperture lenses that can be immersed in water are uncommon and generally possess short working distances, which limit the depth of tissue penetration (i.e., optical sectioning) that can be obtained.

Proper orientation of the tissue specimen is also critical in obtaining flat-field images and is of vital concern when in vivo images are sought from the living eye or other tissues, which are free to move. Alignment of the objective lens in any orientation other than directly perpendicular to the tissue surface results in an oblique optical section through the tissue, which is sometimes difficult to interpret. In practice, perpendicular alignment is usually accomplished for the eye and other living organs by the utilization of dipping cone lenses, which consist of a long working distance objective and cone-shaped tip having either a concave or a flat-front surface and convex posterior surface that is concentric with the axial focal point.^{5,6} Such lenses restrict eye movement and “applanate” by riding directly on a fluid cushion centrally; touch (if any) occurs only at the lateral edges of the field.

PINHOLE DISK AND SCANNING SLIT CLINICAL CONFOCAL MICROSCOPES

In 1968, Petran and coworkers⁹ developed the first scanning confocal microscope using a single white light source and a modified Nipkow disk containing thousands of optically conjugate (source:detector) pinholes arranged in Archimedean spirals (Fig. 1A). Light from a broad-band source passes through the pinholes on one side of the disk and is focused into the specimen. Optically conjugate detector pinholes on the opposite side of the disk prevent light from outside the optical volume, determined by the objective lens and pinhole diameter, from reaching the camera or eyepiece. Rapid rotation of the disk results in even scanning of the tissue in real time. Because the illumination and detection of light through conjugate pinholes occurs in tandem, this microscope was named the tandem scanning confocal microscope (TSCM). This microscope has been configured horizontally for ophthalmic clinic use or vertically for standard laboratory use with placement of the objective lens above or below the specimen. Currently, this microscope is no longer commercially available.

The capabilities of these types of instruments have several major advantages for viewing the living eye and biologic systems: (1) the white light used is not toxic to the tissues scanned and produces minimal discomfort when used on patients or animals¹⁰⁻¹²; (2) real-time images are generated that can be detected by low-light video cameras and viewed directly on a monitor¹³; (3) through mechanical encoding of z-axis position within the objective lens, z-axis position is known and recorded for every (x, y, t) plane observed¹⁴⁻¹⁵; (4) use of diffraction-limited pinholes provides maximal z-axis resolution, and disks of differing hole sizes (20-80 μm) as well as the percentage of transmittance values (number and diameter of holes per disk) can provide optimization of the signal-to-noise ratio for each type and thickness of tissue examined; (5) scanning disk microscopes are also generally cheaper to construct and thus can be purchased at prices well below those of more complex systems; and (6) direct, real-time stereo viewing can be achieved.¹²

Disadvantages of the TSCM system are the current general lack of a wide selection of objective lenses necessary to maximize utilization of potential uses, and the fact that the signal-to-noise ratio cannot be directly varied by altering pinhole size automatically at different tissue depths, a feature available with newer, adjustable scanning slit microscope systems (see below).

TSCMs currently used are horizontally configured on a standard slit-lamp table for routine clinical use (Tandem Scanning Corp., Reston, VA, USA; Advanced Scanning, Ltd.), and employ two specially designed dipping-cone objectives; 24x, 0.6 NA, 0-1.5 mm working distance and 16 x 0.40 NA, 0-8 mm working distance; each objective provides x-y frames of 400 x 400 or 640 x 640 μm , respectively. For the tandem scanning instrument, the position of the focal plane relative to the objective tip is varied by moving the lenses within the objective casing. Lens movement is controlled using an Encoder Mike Controller with a digital read-out interfaced with a personal computer (PC) via a serial port. A program converts the encoder mike reading to the corresponding z-axis position (depth) of the focal plane in micrometers. This number is continuously updated and written into the user bit register of a Time Code Generator via a serial interface. The Time Code Generator writes this number onto the audio track of the super VHS recording; the depth can also be displayed on the video monitor during recording and/or playback. Thus, the depth of the focal plane within the tissue can easily be calibrated, and accurate quantitative four-dimensional imaging is possible with this system.¹⁵ The glass disks contain either 64,000 20- or 30- μm pinholes with total optical transmittances of 0.25 or 0.33%, respectively; disk rotation speed is 900 rotations per minute, which produces "streak-free" images. The light path is composed of prisms and mirrors with a stable and easily maintained alignment. The light source is a 100-W mercury lamp; the instrument is currently approved by the FDA for clinical use in examining the eye.^{11,12}

The axial response of the TSCM system was determined with the 0.6 NA, 24x objective and 0.25% transmittance, 20- μm pinhole disk by focusing through a perfect planar reflector (mirror) and measuring the reflected intensity curve; this yields a z-axis resolution of 9 μm .¹⁴ Lateral x-y resolution in vivo ranges from 0.5 to 1.0 μm .

One important limitation in obtaining high-frame speeds with the TSCM is the dramatic loss in light reaching the tissue, because Nipkow disks transmit only 0.25 – 1% of the available light. This loss of luminance limits the amount of light reflected from low-contrast structures. Thus, a low-light level camera is needed for image acquisition. An additional obstacle to in vivo imaging is that the field of view is often moving owing to pulse, respiration and eye movements. Video frames generated while an object is in motion are often blurred, giving poor resolution of cellular detail. Single frames generated by low-light cameras also suffer from significant noise produced by the image intensifier. A standard technique for reducing the amount of random noise in a single image is to average several sequential frames. However, for image averaging to be successful, the sequential images must be perfectly registered, that is, there must be no positional changes between them. In many in vivo studies, there often is a only a short pause between movements in which the frames are stationary and can be averaged successfully.

These problems have been addressed successfully through the development of a real-time digitizing system that allows the user to step through consecutive digitized frames easily and interactively to align and average sequential frames with adequate registration (to reduce noise) and to save the nonblurred, best quality images. Current system design uses a Pentium PC platform with the high-speed peripheral computer interface (PCI) bus to digitize video signal sequences from either a DAGE-MTI VE camera (DAGE-MTI, Michigan City, IN, USA) or a super VHS recorder¹⁴ directly to the random access memory with utilities for automatic registration, averaging and shading correction of TSCM images (Fig. 1B). The maximum number of sequential images is limited only by the amount of system random access memory on the PC. Some investigators also use the newer CCD cameras and digitize images directly.

In 1994, a new variable-slit real-time scanning confocal microscope (SCCM) was described by Masters and Thae¹⁵ and Bohnke and Masters,¹⁶ which is now available commercially from Nidek Technologies America, Inc. (Greensboro, NC, USA). Mounted on a slit-lamp stand and using a 12-V halogen lamp for noncoherent illumination, the instrument can be used clinically in conjunction with an intensified silicon intensified device (SIT) or charge coupled device (CCD) video camera to examine the living eye.

The optical design of this instrument is similar to the scanning double-sided mirror employed in a real-time laser scanning slit confocal microscope previously developed by Brakenhoff and Visscher¹⁷ and sold commercially by Meridian Instruments (Okemois, MI, USA) (the Insight Microscope). In this design, two independently adjustable slits are located in conjugate optical planes; a rapidly oscillating two-sided mirror is used to scan the image of the slit over the plan of the cornea to produce optical sectioning in real time.

There are two apparent significant advantages inherent in the scanning slit design: (1) by continually adjusting the slit and hence depth of focus in the z-axis, the signal-to-noise ratio can be maximized, ensuring optical image contrast for increasing tissue depths of optical sectioning, (2) the use of a slit provides for higher signal to noise ratio and when used with high numerical aperture objective lenses, the constantly maintained confocality of the adjustable slits produces single video frames of high image clarity. There are also several significant drawbacks to the microscope as currently available. The depth of focus of the scanning slit microscope has recently been determined as 25.9 ± 7.1 microns, which is large when compared to the TSCM, 9 - 12 microns.¹⁸ Thus, there is greater uncertainty in determining the spatial depth of corneal cells and structures. Qualitative measurements of corneal sub-layer depth and thickness also require a special z-ring adapter that is currently available from the manufacturer. This adapter is adequate for most subjects studied, but does not resolve the problem of potential geometric distortion induced by eye measurement within available image scan times (25 Hz).

In the intensified DAGE/MTI VE 1000 SIT camera used with TSCM at video rates, motion often induces blur in some x-y images through persistence of signal in the video camera photo tube from frame to frame. However, even when the SSCM slits are synchronously coupled to the camera (CCD or SIT) chip, and every video frame generated is "clear," eye movement, which is more rapid (30 Hz) will induce geometric distortion in the acquired image, e.g., circles may become ellipses. Because this distortion occurs in three dimensions, the problem is further highlighted. In this situation, when the presence and limits of movements cannot be visualized by eliminating blur sequences, clear images alone are insufficient to validate the actual quantitative localization of all image points observed in the four-dimensional spaces (x, y, z, t) recorded. Thus, the prospective user of confocal instruments, like the modern computer consumer, should be driven by what will fully achieve defined specific performance objectives.

Currently, the only layer of the cornea that can be examined in vivo, noninvasively by a SSCM and not imaged routinely by TSCM is the wing cell layer.¹⁵ If imaging of this structure is critical for the research or clinical questions to be answered, use of the SSCM is indicated. When available, Nipkow disk-based TSCMs, however, provide quantitative routine clinical four-dimensional imaging in real time for all other routine clinical applications.

BACKGROUND REJECTION AND SIGNAL-TO-NOISE OPTIMIZATION IN CONFOCAL MICROSCOPY

In confocal microscopy, narrowly focused light and filtered detection of small volume of object space combine to reduce out-of-focus background light and hence produce an "optical slice" of the specimen examined. In this system, "background" light is defined as detected light that originates within the same volume; volume is geometrically defined by the numerical aperture, magnification, and design of the objective lens itself. Recently, Sandison and Webb¹⁹ rendered an important contribution to the theory and practice of confocal microscopy by measuring background rejection as the signal-to-background ratio (S/B), which is separately calculated for ideal confocal, spinning disk, line-illumination, slit-detection, and conventional fluorescence microscopes as a function of both the spatial filter size (i.e., pinhole diameter or slit width) and specimen thickness. Using this approach, spatial filter sizes that reject background and optimize the signal-to-noise ratio (S/N) are calculated for each type of instrument. To facilitate comparisons, the authors normalized these calculations, such that the time-averaged illumination at each point in the specimen is the same constant for each microscope. For thick specimens (e.g. eye, whole tissues), the S/B ratio obtained by the ideal confocal microscope is >100 times greater than the S/B for conventional microscopy; furthermore, the optimal confocal S/N can be a factor of >10 as well.

Results of these studies comparing S/B and S/N for the different microscopes yield considerable insight into their three-dimensional imaging potential. The "ideal" confocal microscope with a single spot illumination/detection always provides the highest S/B and S/N of microscopes considered. By contrast, real-time spinning disk, pinhole microscopes (TSCM) behave like an ideal confocal microscope as long as the specimen thickness remains less than the hole-to-hole spacing in the disk. With increasing sample thickness, S/B drops an order of magnitude below ideal confocal S/B, but remains much better than conventional microscopy (two to three times greater).

By contrast, the optimized slit-detection microscopy (SSCM) collects more signal than the ideal source/detector TSCM but also collects more background. Therefore, the S/B will be lowest for slit source/slit detector scanning systems, intermediate for point/slit laser scanning fluorescence microscopes, and best for point/point instruments. In practice, this means that in thin tissue samples, due to the confocal-like background rejection of the spinning-disk microscope; the slit detection S/N is only 85% of the spinning disk value. As sample thickness increases, however, in

point/slit detection systems, the S/B ratio decays less rapidly than it does for spinning disk microscopes, and for large thickness values, the resulting slit-detection S/N can be 20% higher than comparable spinning disk values.¹⁹

As stated by the authors, the practical summary of this approach is the critical realization that “no microscope dominates in every imaging situation, and none is always deficient”.¹⁹ Thus, each type of source/detector design instrument will seek the biologic problems whose spatial and temporal resolution are optimally addressed by the inherent trade-off between background rejection and imaging speed.

IN VIVO LASER SCANNING CONFOCAL MICROSCOPY

Recently, a new, coherent in vivo confocal microscope has been developed for clinical use in the cornea by Heidelberg Engineering GmbH, Dossenheim, Germany.²⁰⁻²¹ This microscope is a low-cost add-on module to that manufacturer’s optic nerve and retinal laser scanning microscope. This system uses a 63x 0.95 NA, wd 1.45 Zeiss (Germany) water-immersion objective lens, with a 670-nm diode laser as a point light source and covers a 400 x 400 micron area of observation. This lens is coupled to the cornea via a polymethylmethacrylate cup with interposition of a transparent lubricating gel (Vidisc, Mann-Pharma, Germany) for in vivo imaging. For 3-dimensional data acquisition, an internal scanning device moves the focal plane perpendicular to the x-y plane. Coupling provides control of eye movements. As expected using coherent light, this new microscope provides exquisite images of all corneal and other ocular surface cells and substructures. For the first time, optically-sectioned images of high-spatial resolution are possible for the bulbar and palpebral conjunctiva, meibomian glands, Langerhans cells (density and distribution) as well as all corneal cell layers and substructures.²²⁻²³ The current major disadvantage of this system, however, is the inability to perform real-time automated through-focus of all corneal layers with on-line 3D reconstruction with the current objective lens. This problem could be solved by straightforward engineering improvements.

QUANTITATIVE THREE-DIMENSIONAL CONFOCAL IMAGING OF THE CORNEA IN VIVO

The eminent Cornell University physicist Watt Webb once remarked that “although one confocal picture was worth a thousand words, one number was worth a thousand pictures,” (Webb, 1988, personal communication). This highlights one of the major thrusts of in vivo imaging research in the eye in the past quarter century: the need to go from pictures to numbers. Nowhere is this problem more evident than in the clinical and research need to measure rapidly, accurately, and reproducibly the sublayer thickness and cellular layer population (area, shape, number) four dimensionally (s, y, z, t) in the in situ living cornea.

To meet this critical need, a powerful new technique called confocal microscopy through-focusing (CMTF) was recently developed.²⁴ CMTF is the operation of rapidly moving the focal plane through the cornea in real-time, resulting in a 3-D stack of 400-500 two-dimensional images. From this stack, a z-axis intensity profile is generated by calculating the average pixel intensity in a central region of each image and plotting versus z-depth. This approach takes advantages of the mechanical advance mechanism for the internal lens elements, which can be set by the Oriel encoder to a specific speed to facilitate fast or slow focusing through the tissue. While advancing the lens elements and simultaneously video recording the images, the axial distance between consecutive video frames can be calculated based on the lens advance speed. For the current system, a lens advance speed of 80 $\mu\text{m/s}$ translates to an axial distance of -1.06 μm between consecutive images. Using this approach, approximately 15 seconds are required to focus through and capture the entire corneal thickness. This speed can be increased to 160 $\mu\text{m/s}$ without loss of axial resolution owing to the interlacing of video lines from the DAGE/MTI camera, albeit at the expense of horizontal resolution. At this higher speed, recording of the entire cornea only takes approximately 8 seconds; whereas, the corneal epithelium can be captured in less than one second, substantially reducing the risk of axial drift interfering with thickness measurements. Furthermore, multiple scans through the cornea, or just the corneal epithelium, can be performed rapidly and easily for a more accurate measurement of tissue thickness.

Digitizing the through focus scan and reconstructing the cornea three dimensionally produces a cross-sectional (x-y) view of the living cornea that appears similar to that of histologic sections (Figs 2-3). Furthermore, the relative thickness of the corneal epithelial sheet and stroma as defined by the respective separation between the superficial epithelium (Epi) and basal lamina (BL) and the basal lamina and endothelium (Endo) appears equivalent to that observed histologically. Although thickness measurements from the surface projection are possible, an axial, light-scattering profile can be calculated by measuring the average pixel intensity of each image comprising the through-focus scan and plotting as a function of axial depth (Fig. 2). This representation identifies the major tissue structures that backscatter or reflect light as peaks in the depth-intensity profile. Interestingly, tissue interfaces between cells and matrix (epithelium and stroma) or tissues and fluid (tears or anterior chamber aqueous), where there are changes in the refractive index, appear to be the major source of backscatter.

Using the two-dimensional depth-intensity profile, tissue thickness can be measured objectively, without operator bias, by measuring the distance between the intensity peaks. For the cornea, the corneal thickness (CT), epithelial thickness (ET), and stromal thickness (ST) can be calculated using the following equations:

$$CT = Z_{\text{endo}} - Z_{\text{epi}}; ET = Z_{\text{bl}} - Z_{\text{epi}}; ST = Z_{\text{endo}} - Z_{\text{bl}},$$

where Z_{epi} , Z_{bl} , and Z_{endo} are the axial depths of the intensity peaks for the superficial epithelium, basal lamina, and endothelium, respectively. For the rabbit, these thicknesses have been determined to be $381.6 \pm 27.3 \mu\text{m}$, for the corneal thickness and $47.7 \pm 2.2 \mu\text{m}$ for the corneal epithelial thickness in a series of 10 rabbits, which is in agreement with the known thickness of these structures using other techniques.²⁴ For the corneal epithelium, the standard deviation of repeat scans ranged from 1.3 to 3.1 μm with a coefficient of variation of 2.5%, suggesting that this method is reproducible and accurate. For human patients, similar accuracy and repeatability have been reported, and intracorneal structures as small as 16 μm (Bowman's membrane) have been measured reproducibly.

In addition to measuring sublayer thickness, CMTF analysis also provides a simple quantitative means of studying tissue responses in four dimensions. This has been demonstrated in studies of corneal wound healing after excimer laser keratorefractive surgery in which a portion of the anterior cornea is photoablated, changing the central corneal curvature.²⁵⁻²⁸ Using CMTF image data sets, the same cornea can be reconstructed three dimensionally at various times before and after surgery (Fig. 3). By comparing the images from one time point to another, the immediate loss of corneal tissue can be quantified and the effects of laser ablation and later tissue responses can be studied. Finally, CMTF profiles can also be used to estimate the amount of backscattering of light from the tissue.²⁹ If the camera gain, KV, and black level are set to constant levels, then the amount of light detected by the camera is principally related to changes in the reflectivity or backscattering of light by the tissue. Relative light backscattering can then be estimated by integrating the area under each peak or the entire curve; the unit of measurement (U) is defined as $\mu\text{m} \times \text{pixel intensity}$. Using this method, a close correlation between the loss of corneal transparency, as measured by the clinical examination of the cornea, and the CMTF estimate of light backscattering was shown (Fig. 3). Furthermore, integration of the CMTF intensity peak can also be used to evaluate ocular irritation and to provide an objective, quantitative measure of the corneal response to injury, including inflammation, fibrosis, and repair. Although the pixel intensity values do not by themselves indicate any specific response, values can be correlated directly to actual images taken during scanning to identify unique pathologic processes underlying the elevated intensities.²⁵⁻²⁸ Integration of intensity values over a region of the cornea, i.e., stroma, then allows objective quantitative measure of the area and depth of response occurring within the same tissue.

Unfortunately, it is just becoming possible to apply this new method quantitatively to the scanning slit microscope (Nidek, USA). Although through-focus scan images can be generated in SSCM, owing to the lack of a suitable variable focus, dipping cone objective, there is currently no reliable ability to locate sublayer structures relative to a known zero point for all patients, and there is no possible compensation for the geometric distortion problem induced by movement. These problems are currently being addressed by the manufacturer.

HIGHER ORDER HARMONIC AND MULTI-PHOTON IN VIVO IMAGING

There has been recent widespread appreciation of the powerful insights provided by non-linear physical phenomena in medicine and cellular biology. The most widespread and robustly developed applications are currently found in fluorescence microscopy. The two most important of these non-linear methods are multi-photon (MP) and higher order (2nd, 3rd, etc) harmonic imaging (HHI). Both can be adapted to in vivo clinical use; used together, each provides complementary structural information.³⁰⁻³²

Simultaneous multiphoton absorption by a fluorophore or other molecular target (fluorescein, Q-dot, or other chromophore) is based on non-linear absorption of exciting light with resultant signaling and chromophore location, a non-coherent process. By contrast, second or higher order harmonic imaging relies upon non-linear forward or backscattering and does not involve an excited state but is a coherent process. Both MP and HHI provide optical sectioning deep within target cells and tissues with inherent 3-dimensional capability. For both techniques, the exciting, incident, wavelengths lie in the infrared, providing less scattering and deeper penetration into the cornea or other target tissues. Disadvantages of MP and HHI are poorer spatial resolution and contrast when compared to conventional one-photon confocal imaging. However, this disadvantage may be balanced by the observation that along the z-axis, excitation of the target tissue is confined to a very small region in the focal plane due to the quadratic dependence of excitational energies on the excitation-induced photon flux by both modalities. Thus, "out-of-focal-plane" photobleaching and phototoxicity are greatly reduced, which should facilitate valuable clinical in vivo use.

Since HHI does not arise from an absorptive process, under symmetry constraints, HHI can most efficiently be observed at biological interfaces, where tissue-symmetry breaks, where a large change in tissue-refractive index occurs

or where sub-structures are present that have a high degree of orientation and organization but lack inversion symmetry. Such characteristics are ideal for the visualization of endogenous collagen structure in the highly-ordered fibrillar matrix of the cornea. Recently, Jester et al (2005)³² reported the first use of HHI in the human, chicken, mouse, and rabbit corneas. HHI from unstained chicken corneas showed a highly ordered, orthogonal arrangement of collagen bundles forming a lattice network that rotated 200 degrees within the anterior 50% of the cornea. By contrast, mammalian corneas exhibited an anterior interwoven pattern of narrow collagen bends and a posterior orthogonal pattern of broad, parallel bands. This latter pattern was most prominent in the human cornea where backscatter signals showed an amorphous pattern from the most anterior cornea corresponding to Bowman's layer, but a complex interwoven pattern in the deeper stromal matrix. Interestingly, collagen lamellae which exhibited strong forward scattering showed weak backscattering that was seen as spaces between collagen bundles. Many of these strong, forward-scattering lamellae appear to run tangential to the corneal surface and can be detected as voids within backscatter images. An elegant combination of MP and HHI elucidating the structure and function of nematode neurons has also been reported by Filippidis et al (2003).³⁰ It is thus clear that both MP and HHI have an important future in being adapted to in vivo use.

CHALLENGES FOR NEEDED FUTURE IMPROVEMENTS

Perhaps the most important past and continuing disappointment to devotees of the emerging in vivo imaging community has been the extraordinary slowness between theoretical conception of new microscope paradigms and technological translation to actual use by clinicians or research scientists. Petran envisioned the first TSCM in the 1960s, but the first clinical prototype was not built and used until 1988. Webb reported the feasibility of MP microscopy in 1990.³³ The first instruments for in vitro use only became available more than a decade later. In assessing the reasons for this and the continuing slow development of ocular clinical applications in in vivo imaging, three principal factors appear to emerge: cost, lack of platform suitability for specific applications, and lack of internally focusable, long-working distance, water immersible objective lenses that appanate the eye (reduce motion). It appears clear that coherent light confocal imaging offers better resolution than white-light imaging, particularly for red-wavelength sourcing. The ideal in vivo confocal microscope would thus appear to be the Heidelberg II Cornea Module with a mechanized scan capable of real-time (30 Hz) through-focus collection of x-y sections and on-line 3-dimensional reconstruction in real time. Alternatively, the performance of the SSCM could be greatly improved by a contact objective with internal focusing similar to that of the TSCM. Finally, development of a slit-lamp mounted platform and optics for a HHI microscope is clearly a high priority for clinical use.

SUMMARY

New bioimaging methods have played a key role in important new discoveries in corneal structure and function in the past 25 years. Disease or change can be followed noninvasively in situ as they occur. The success of treatment or the toxic effects of pharmacological intervention can be directly monitored in individual patients. Wound healing can be studied sequentially and adverse scarring or tissue reaction localized, quantitated and characterized at the subcellular level. This powerful approach has the potential to transform the safety and efficacy of excimer laser refractive surgery, and with further development and applications, all the pathobiology of the eye.

Subsection Heading: Ophthalmic Technologies, XVI.

Acknowledgement: Supported in part by EY-10738, Ey-0166634, The Pearle Vision Foundation, Dallas, TX, the Lew Wasserman Award (WMP), and an institutional research grant from Research to Prevent Blindness, New York, NY

References

1. Minsky M. Memoir on inventing the confocal scanning microscope. *J Scanning* 1988;10:128–38.
2. Wilson T, Sheppard C. *Theory and practice of scanning optical microscopy*. London: Academic Press, 1984.
3. Sheppard CJR, Cogswell CJ. Optimization of the confocal microscopy system. *Trans R Microsc Soc* 1990;1:231–4.
4. Maurice DM. A scanning slit optical microscopy. *Invest Ophthalmol* 1974;13:1033–7.
5. Bourne WM, McCarey BE, Kaufman HE. Clinical specular microscopy. *Trans Am Acad Ophthalmol Otolaryngol* 1976;81:743–53.
6. Koester CJ. Scanning mirror microscope with optical sectioning characteristics: applications in ophthalmology. *Appl Optics* 1980;19:1749–57.

7. Koester CJ, Auran JD, Rosskothén HD, et al. Clinical microscopy of the cornea using optical sectioning and a high numerical aperture objective. *J Opt Soc Am* 1993;10:1670–9.
8. Koester CJ, Auran JD, Rapaport R, et al. Confocal scanning slit microscopy of normal human corneal basal epithelium centripetal slide and presumed Langerhans cell movement. *Invest Ophthalmol Vis Sci* 1993;34(suppl);1014.
9. Petran M, Hadravsky M, Egger MD, et al. Tandem-scanning reflected-light microscope. *J Opt Soc Am* 1968;58:661–4.
10. Cavanagh HD, Jester JV, Essepian J, et al. Confocal microscopy of the living eye. *CLAO J* 1990;16:65–73.
11. Cavanagh HD, Petroll WM, Alizadeh H, et al. Clinical and diagnostic use of in vivo confocal microscopy in patients with corneal disease. *Ophthalmology* 1993;100:1444–54.
12. Cavanagh HD, Petroll WM, Jester JV. Confocal microscopy: uses in measurement of cellular structure and function. *Prog Retinal Eye Res* 1995;14:527–65.
13. Petroll WM, Jester JV, Cavanagh HD. In vivo confocal imaging. *Int Rev Exp Pathol* 1996;36:93–129.
14. Petroll WM, Cavanagh HD, Jester JV. Three-dimensional imaging of corneal cells using in vivo confocal microscopy. *J Microsc* 1993;170: 213–9.
15. Masters BR, Thaeer AA. Real-time scanning slit confocal microscopy of the in vivo human cornea. *Appl Optics* 1994;33:695–701.
16. Bohnke M, Masters BR. Confocal microscopy of the cornea. *Prog Retinal Eye Res* 1999;18:553–628.
17. Brakenhoff GJ, Visscher K. Confocal imaging with bilateral scanning and array detectors. *J Microsc* 1992;165:139–46.
18. McLaren JW, Nau CB, Kitzmann S, et al. Keratocyte density: comparison of two confocal microscopes. *Eye and Contact Lens* 2005;31:28-33.
19. Sandison DR, Webb WW. Background rejection and signal-to-noise optimization in confocal and alternative fluorescence microscopes. *Appl Optics* 1994;33:603–15.
20. Stave J, Zinser G, Grummers G, et al. Modified Heidelberg retinal tomograph HRT. Initial results of in vivo presentation of corneal structures. *Ophthalmology* 2002;99:276-280.
21. Heidelberg Retina Tomograph II, (Rostock Cornea Module). Operating Instructions of Software, version 1.1. Dossenheim, Germany, 2004.
22. Zhivov A, Stave J, Vollmer B, et al. In vivo confocal microscopic evaluation of Langerhans cell density and distribution in the normal human corneal epithelium. *Graefe's Arch Clin Exp Ophthalmol* 2005;243:1056-1061.
23. Kobayashi A, Yoshita T, Sugiyama K. In vivo findings of the bulbar/palpebral conjunctivitis and presumed meibomian glands by scanning confocal microscopy. *Cornea* 2005;24:985-988.
24. Li HF, Petroll WM, Moller-Pedersen T, et al. Epithelial and corneal thickness measurements by in vivo confocal microscopy through focusing (CMTF). *Curr Eye Res* 1997;16:214–21.
25. Moller-Pedersen T, Li HF, Petroll WM, et al. Confocal microscopic characterization of wound repair after photorefractive keratectomy. *Invest Ophthalmol Vis Sci* 1997;39:487–501.
26. Moller-Pedersen T, Vogel M, Li HF, et al. Quantification of stromal thinning, epithelial thickness, and corneal haze after photorefractive keratectomy using in vivo confocal microscopy. *Ophthalmology* 1997; 104:360–8.
27. Moller-Pedersen T, Cavanagh H, Petroll WM, et al. Corneal haze development is regulated by volume of stromal tissue removal. *Cornea* 1998;17:627–39.
28. Moller-Pedersen T, Cavanagh HD, Petroll WM, et al. Neutralizing antibody to TGF β modulates stromal fibrosis but not regression of photoablative effect following PRK. *Curr Eye Res* 1998;17:736–47.
29. Jester JV, Moller-Pedersen T, Huang J, et al. The cellular basis of corneal transparency: evidence for “corneal crystals.” *J Cell Sci* 1999;112:613–22.
30. Filippidis G, Kouloumentas C, Voglis G, et al. Imaging of *Caenorhabditis elegans* neurons by second-harmonic generation and two-photon excitation fluorescence. *J Biomed Optics* 2005;10:024015.
31. Ficke M, Nielsen T. Two-dimensional imaging without scanning by multiphoton microscopy. *Appl Optics* 2005;44:2984-2988.
32. Jester JV, Morishige N, Cavanagh HD, Svoboda K, Petroll WM. Probing tissue structure by second harmonic generated signals. *Focus Microscopy* 2005, 19th Yearly Conference, Friedrich Schiller Univ, Jena, Germany, March 20-23, Abstract, p. 66.
33. Denk W, Strickler JH, Wells WW. Two-photon laser scanning fluorescence microscopy. *Science* 1990;248:73-76.

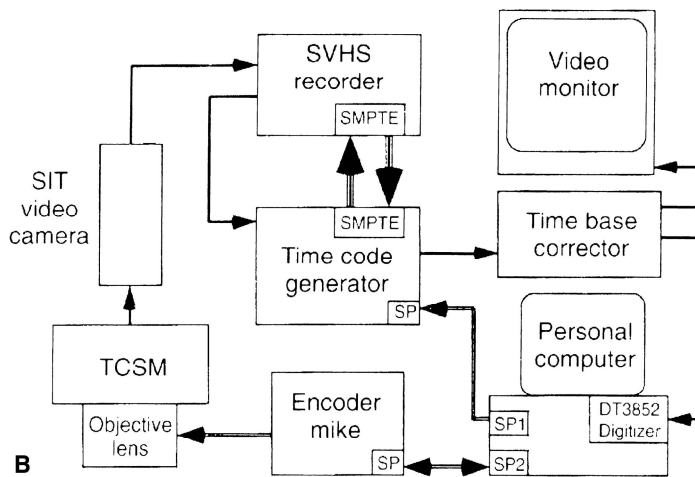
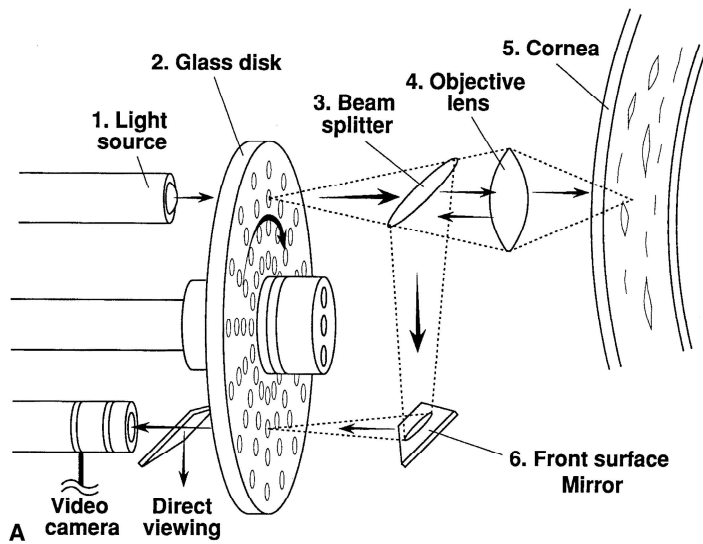


Fig. 1. A: Design and light path of the TSCM. **B.** The system hardware configuration for image acquisition, digitization, processing, display, and storage in CMTF.

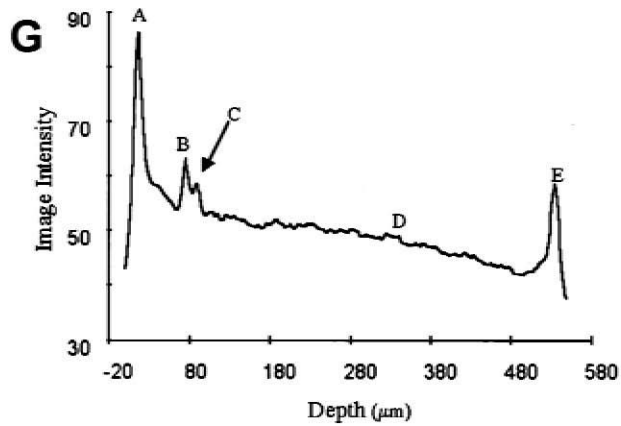
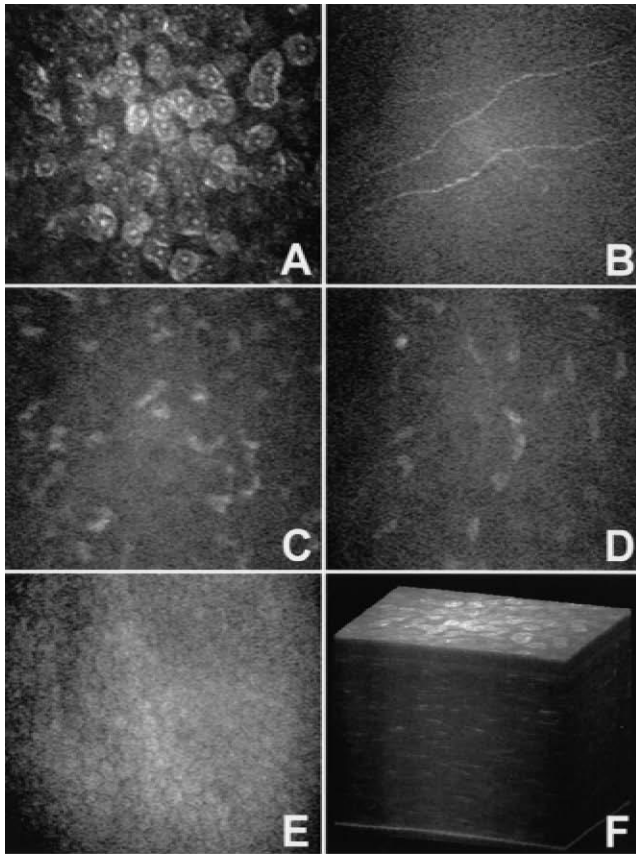


Fig. 2. Corneal images digitized directly from a CMTF scan (A-E) and the corresponding CMTF intensity curve (panel G) in a human volunteer. **A:** Epithelial image corresponding to peak A. **B:** Basal-epithelial nerve plexus image corresponding to peak B. **C:** Image of anterior layer of keratocyte nuclei corresponding to peak C. **D:** Stromal image corresponding to peak D. **E:** Endothelium image corresponding to peak E. **F:** Three-dimensional reconstruction. **G:** CMTF intensity curve. Horizontal field width in A-E, 330 μm . Reprinted with permission from *Curr Eye Res*¹⁹ Copyright 1997, Swets & Zeitlinger.

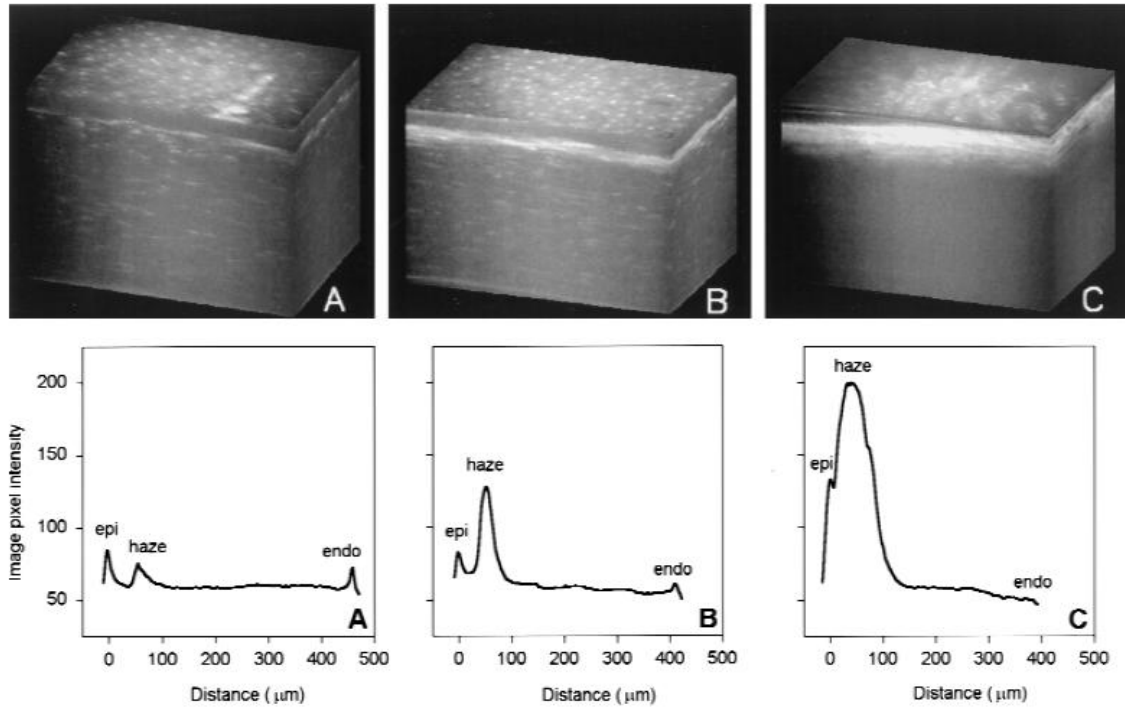


Fig 3. Three-dimensional reconstructions and corresponding CMTF scans of three human corneas 1 month after PRK. **A:** A clinically clear cornea (grade 0 haze). **B:** Cornea with clinical grade 2 haze. **C:** Cornea with clinical grade 4 haze. Note the increased subepithelial reflectivity in all three corneas. In the corresponding CMTF scans, a profound increase in both haze thickness (haze peak width) and haze intensity (haze peak height) is seen with increasing clinical grades. Reprinted with permission from *Invest Ophthalmol Vis Sci*.³⁷ Copyright 1997, the Association for Research in Vision and Ophthalmology.